IMU-Based Gait Event Detection in Real-World Settings:

Comparative Evaluation of Sensor Placements and Detection Algorithms

by

Romin Gaalman

in partial fulfillment of the requirements to obtain the degree of

Master of Science in Biomedical Engineering

at the Delft University of Technology

to be defended publicly on **26 May 2025 at 09:30**

Thesis committee

Dr. ir. Eline van der Kruk	(chair)
Ir. Koen Jongbloed	(daily supervisor)
Dr. ir. Winfred Mugge	(external examiner)

Student number: 5185475
Faculty: Mechanical Engineering

TU Delft

IMU-Based Gait Event Detection in Real-World Settings: Comparative Evaluation of Sensor Placements and Detection Algorithms

Abstract: Gait event detection (GED) plays an important role in clinical gait analysis and rehabilitation. Real-time detection of temporal gait features within the gait cycle is essential for closed-loop control of wearable assistive devices and neuroprostheses. Machine-learning algorithms used in these systems require training datasets of real-world walking, which are currently collected using insole footswitches. However, insole footswitches suffer from performance and reliability issues. This study evaluates the use of inertial measurement units (IMUs) as an alternative for detecting foot-ground contact events during gait. The detection performance of five IMU placement locations and four rule-based detection algorithms was assessed in laboratory and real-world settings, using force plates and footswitches as ground-truth reference. In the laboratory, the heel-mounted IMU combined with a vertical jerk–based algorithm achieved an F1-score of 97.6% and a mean timing error of –1.5 ± 1.5 ms relative to force plates. Although insole footswitches achieved a comparable F1-score (97.2%), they showed significantly larger timing errors (17.7 ± 11.7 ms, $p < 0.001$). In the real-world environments, the heel-mounted IMU combined with a zero-velocity update–based detection algorithm achieved a mean timing error of –5.0 ± 23.4 ms relative to the footswitches. These findings show that a single heel-mounted IMU combined with a rule-based detection algorithm offers a practical and accurate alternative to insole footswitches for collecting gait datasets in real-world environments.

Keywords: Wearable Assistive Devices; Gait Event Detection; Inertial Measurement Unit

1. Introduction

Gait analysis, the quantitative study of human locomotion, is a valuable clinical tool for diagnosing gait disorders and monitoring rehabilitation progress [1–3]. Recent technological advancements have enabled out-of-lab gait analysis using wearable sensor-based gait event detection (GED) systems [4–7]. These systems combine hardware and software to identify events in the gait cycle, which can provide insights into walking patterns in real-world environments [4,8]. Furthermore, wearable GED systems are applied in assistive devices and neuroprostheses to facilitate closed-loop control [9]. An example of a wearable assistive device that uses GED is the Biostim shorts, developed by the company Biomex (Figure 1). The shorts aim to correct compensatory movement patterns during gait in real-time using functional electrical stimulation (FES). The delivery of the stimulation in gait-specific FES must occur within a narrow intervention window to be effective [10,11]. Therefore, accurate and temporally precise GED is critical for gait-specific FES in wearable assistive devices FES [4,12,13]. The GED system embedded in the Biostim shorts includes two inertial measurement units (IMUs) positioned within lateral thigh compartments to capture motion data. These data are processed in real time by a machine-learning-based GED model. The training and validation of these ML GED models require extensive datasets of walking patterns in real-world environments. Currently, the only wearable sensors used for the collection of these datasets are insole pressure sensors, also known as footswitches [4].

Footswitches typically consist of one or multiple force-sensing resistors (FSRs), embedded in the insole. The force exerted on the FSRs by the foot during stance affects their conductance, from which the foot-ground contact timing can be determined. However, several limitations affect the accuracy and reliability of the footswitches for foot-ground contact detection. Moreover, the FSR conductivity is also affected by the insole shape, its surface compliance and temperature [14]. Therefore, the selection of appropriate force thresholds is challenging. Low thresholds may trigger false positives, while high thresholds can result in

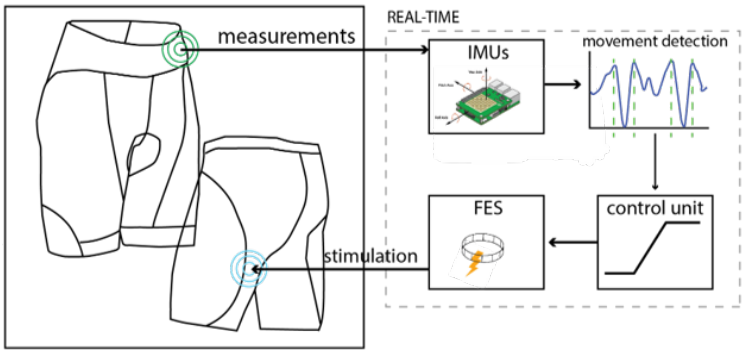

Figure 1. Schematic of the Biostim shorts developed by Biomex Ltd. The arrows illustrate the working mechanism: inertial measurement units (IMUs) capture motion data, gait events are detected, and the control unit processes the signals to trigger functional electrical stimulation (FES). Schematic reproduced with permission from Biomex Ltd.

false-negative detections [15]. Threshold tuning is further complicated by inter-individual differences in body weight and clinical conditions. Finally, insole footswitches have been reported to cause discomfort and may alter natural gait patterns, which limits their suitability for prolonged use in real-world settings [16]. In contrast, IMU-based detection systems do not suffer from these issues because they are wireless and can be unobtrusively positioned without causing discomfort during prolonged use. Previous studies have demonstrated high detection performance for initial contact (IC) when using IMUs placed on the feet and for toe-off (TO) when using IMUs placed on the shank [17,18]. Besides the temporal detection of foot-ground contacts, IMU-based systems can be used to capture more comprehensive movement data. For instance, the detection of gait events within the swing phase [6,19] and estimate spatiotemporal parameters such as minimal foot clearance during mid-swing [20].

The practical advantages and broader applications of IMU-based systems raise the question if IMU-based GED could be a viable alternative to insole footswitches for collecting labeled training datasets in real-world settings. Therefore, the aim of this study is to design and evaluate an IMU-based GED system for collecting training datasets in real-world environments. To achieve this, gait data are collected using insole footswitches and lower-leg worn IMUs, in both laboratory and real-world environments. The detection performance of insole footswitches and multiple combinations of IMU-placement locations and detection algorithms is assessed using force plate ground truth. Additionally, the GED performance of these IMU-based GED systems is evaluated in real-world environments using insole footswitches as ground truth reference. Although previous studies have validated the detection performance of both IMU-based GED systems and footswitches in laboratory settings using force plate ground truth [17,21,22], no studies have subsequently evaluated the performance of IMU-based GED systems in real-world environments using footswitches as the reference. If IMU-based GED systems meet the performance requirements for collecting real-world training data, it could provide a more practical and comprehensive method for the collection of training datasets. This in turn would benefit training of the ML-algorithms and enhance the performance of assistive wearable devices.

2. Materials and Methods

2.1. Participants

The study was conducted in and around the human motion capture laboratory at Delft University of Technology and approved by the university's Human Research Ethics Committee. Four healthy adults (three females, one male; ages 31, 34, 64, and 67 years; heights 164.5, 166.4, 172.5, and 177.3 cm; weights 64.7, 79.1, 72.4, and 81.6 kg) participated in the study. Participants were recruited via email and through local inquiries. Prior to participation, participants were familiarized with the experimental protocol and provided written informed consent. After recording height and weight, participants were provided with Biostim shorts in multiple sizes and instructed to wear the best-fitting size.

2.2. Instrumentation

Each participant's right shoe was fitted with an insole footswitch containing two FSRs (Odstock Medical, Figure 2a,b). The insole was inserted into the shoe bed so that its FSRs were aligned beneath the calcaneus and the first metatarsophalangeal joints. Additionally, two IMUs (Cometa MiniX) were attached to the midpoint of the shoe's heel and instep (Figure 2e) and three IMUs were placed on right shin using the medial condyle and medial malleolus as anatomical landmarks to ensure standardized placement. The medial side of the shank was selected because the flat, hard surface of the tibia minimizes soft-tissue wobble artifacts. Each sensor was oriented so that its z-axis was aligned with the tibia's longitudinal axis. The upper shin IMU was positioned approximately 5 cm below the medial condyle, the lower shin IMU about 5 cm above the medial malleolus, and the third shin IMU was installed midway between these two sensors. The IMU system was connected to five force plates (Kistler 9260AA) via the Qualysis data acquisition system for synchronized data collection at a 500 Hz sampling rate. Synchronization of the footswitch system with both the IMUs and force plates was achieved by transmitting a sync-out signal from the Qualysis system to the Biostim control unit.

Figure 2. (a) A single force-sensitive resistor (FSR; Odstock Medical). (b) Insole footswitch system with two embedded FSRs and connecting cables. (c) Biostim shorts with control unit and thigh IMUs. (d) Participant wearing the Biostim shorts, with visible footswitch cables. (e) IMU placements on the shin and shoe.

2.3. Procedure

The first part of the experiment was conducted on an 8-m walkway with force plates positioned at the midpoint. Participants walked back and forth until approximately 25 right-foot steps were recorded, completing two trials at a self-selected preferred walking speed (PWS) and two trials at a fast pace. They were instructed to walk at their typical pace for the PWS trials and to walk briskly without running for the fast-paced trials. The second part of the experiment was set up to resemble real-world walking conditions, with the footswitches serving as the ground truth reference. Participants were guided through the laboratory building to the exit at their PWS, avoiding obstacles as they normally would. Once outside, participants walked along a straight section of a sidewalk and then returned via the same route under the fast-paced walking speed condition. Each participant completed a total of four trials in the laboratory and a single trial longer duration in real-world environments, due to limitations in measurement duration of the Biostim system used for the footswitch data (maximum recording duration of 16 minutes per trial).

2.4. Data Processing and Event Detection

All data processing and analysis were performed in MATLAB R2024b. The identification of the HS, TO, and synchronization timestamps from the footswitch recordings was based on changes in the FSR outputs. Specifically, heel-ground and forefoot-ground contacts were detected by respective signal shifts of -64 and -128 from the baseline in the 8-bit analog-to-digital (0-255) range. After identifying HS and TO candidates, duplicate and spurious events were removed based on their temporal proximity and verified by visual inspection of the signal 3(**a**)). For example, when two HS events were detected within 0.02 s, the first HS event was retained as valid for that step. If no TO was recorded between two consecutive HSs, the heel-off event

was marked as the TO for that step. Lastly, each recording was trimmed to the synchronization timestamp, aligning the start times of all measurement devices. The force plate foot-ground contact events were derived

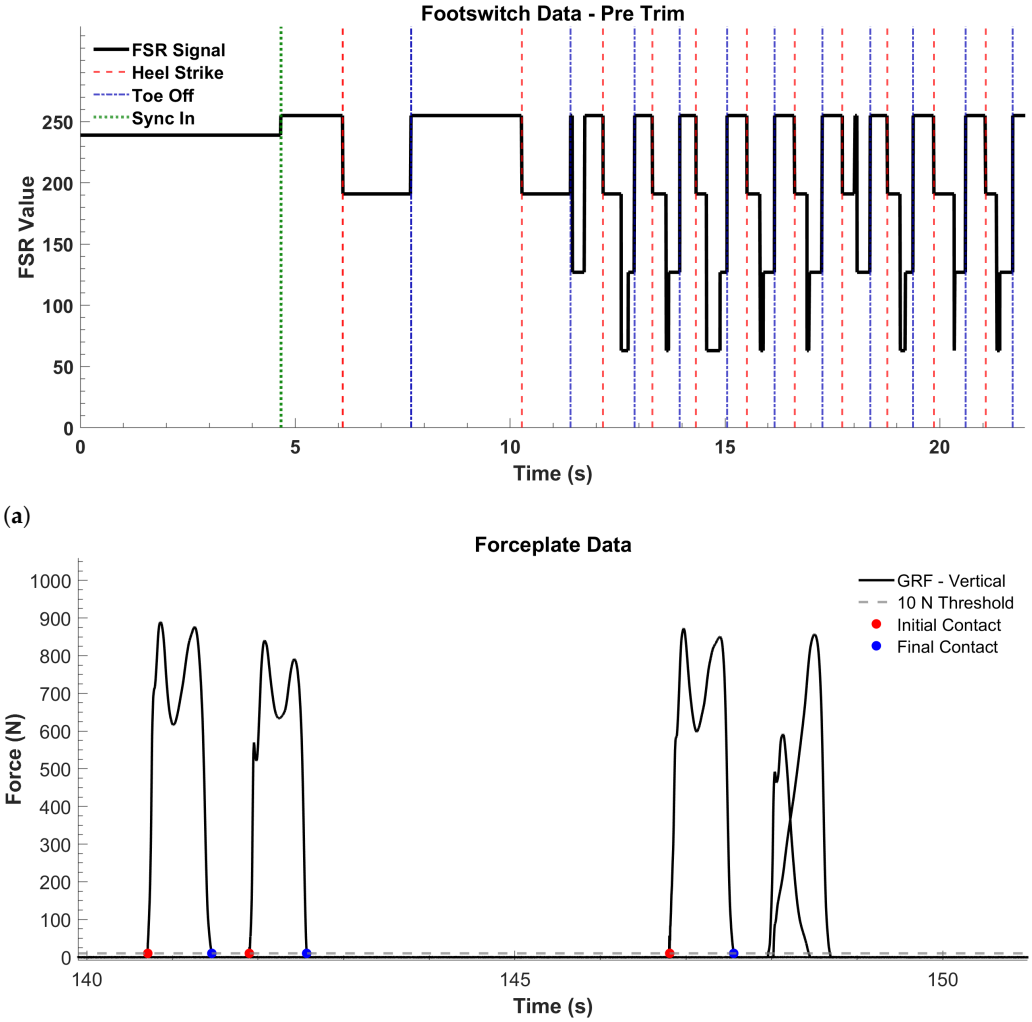

Figure 3. (a) Footswitch recording from a real-world walking trial, prior to synchronization trimming. The synchronization timestamp, heel–strike (HS) and toe-off (TO) events are marked by vertical dashed lines. For strides with a false-negative TO detection, the heel-off was used as the TO for that stride. (b) Vertical ground reaction force (GRF) recording from force plates during the laboratory trials. Four right-foot steps are shown with initial contact (IC) and final contact (FC) marked; the fourth step was excluded because it was captured across two plates.

from the unfiltered vertical ground reaction forces, shown in Figure 3(**b**). Because force plate-based methods cannot differentiate between heel and forefoot contact, the terms initial contact (IC) and final contact (FC) are used for foot-ground interactions detected with the force plates. Previous studies have used force thresholds ranging from 2.5 N to 50 N for force plate-based IC detection [15,23–25], with 10 N being the most commonly used threshold [26–28]. Although lower force thresholds can approximate the IC timing more precisely, they also result in higher false positive detection rates due to noise and vibrations. Therefore, a 10 N force threshold was selected for IC event detection. Duplicate detections were filtered using a 0.3 s minimum separation rule of consecutive ICs. Steps that were not fully captured by a single force plate were excluded.

2.5. IMU Processing

Prior to implementation of the IMU-based detection algorithms, the IMU-data was preprocessed as follows. First, the recordings were transformed to the inertial coordinate system using the direction of the gravitational acceleration vector, recorded while participants were standing in place. Subsequently, the gravitational component was subtracted from the vertical acceleration signal. This was done to mitigate the

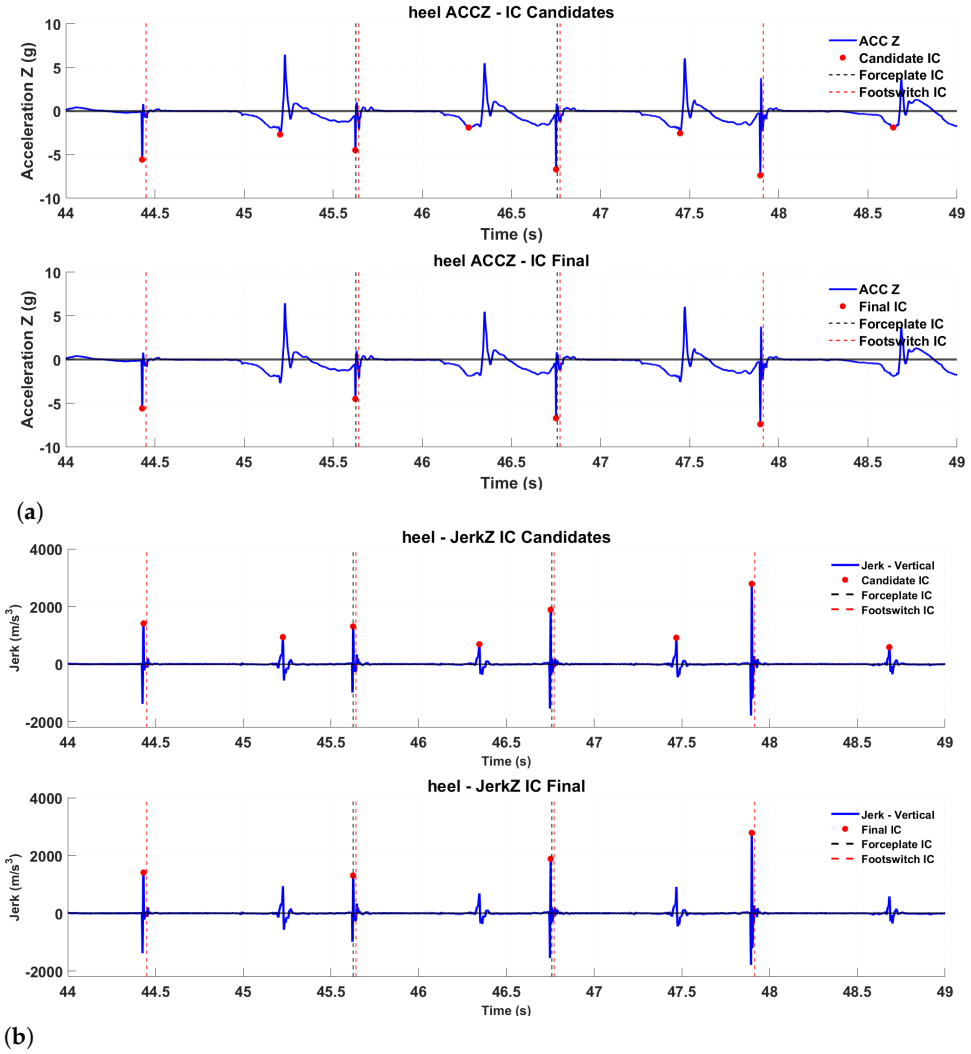

Figure 4. IMU-based initial-contact (IC) detection using the ACCZ algorithm (a) and the JERKZ algorithm (b). The ACCZ algorithm identifies ICs using local minima in the vertical acceleration signal. The JERKZ algorithm detects ICs based on local maxima in vertical jerk. In both panels, vertical dashed lines indicate reference ICs from footswitches (red) and force plates (black). The red dots indicate candidate ICs in the top subplots, in the bottom subplots the remaining ICs after the second pass.

effects of variations in sensor alignment on the detection performance. No additional filtering or smoothing was applied during processing.

A literature search was conducted to identify existing rule-based IC detection methods. Four detection

Table 1. Overview of IMU-Based Gait Event Detection Algorithms used and related works

Algorithm	Target Variable	Method	Ref
ACCZ	Acceleration - Vertical	Peak Detection (Minima)	[17]
JERKZ	Jerk Vertical	Peak Detection (Maxima)	[15]
ZUPT	Angular Velocity - Sagittal	Zero-velocity interval & Peak Detection	[17,29,30]
ZUPT-CROSS	Angular Velocity - Sagittal	Zero-velocity interval & Zero-crossing	

algorithms were developed based on these works, each was adapted to accommodate all placement locations used in this study. Furthermore, the parameters of each algorithm were tuned to achieve reliable IC detection across walking environments and speed conditions. The detection algorithms were named based on the target variable or method used for IC detection. Table 1 presents the four detection algorithms, ACCZ, JERKZ, ZUPT and ZUPT-CROSS, along with the studies that employed similar methods.

The ACCZ algorithm identifies ICs by detecting local minima in the vertical acceleration signal, which result from the rapid deceleration of the lower leg during the swing-to-stance transition. A two-step approach distinguishes these minima from those at mid-swing (Figure 4(**a**)). n the first pass, all local minima in each trial are identified using MATLAB's findpeaks function (MinPeakProminence 0̄.4 and MinPeakDistance =0.3) and marked as candidate IC events. In the second pass, mid-swing and other invalid candidates are removed based on two criteria: the peak width at half-amplitude must be less than 30 ms and the interval between consecutive candidates must range from 0.45 to 2 s. If a candidate IC occurs within 0.45 s of a previous candidate and is more negative, it replaces the earlier candidate.

Instead of the vertical acceleration, the JERKZ algorithm uses its first time derivative, jerk, as the target variable. Since jerk reflects the rate of change of acceleration, the pronounced minimum in vertical acceleration at IC produces a distinct local maximum in the jerk signal (Figure 4(**b**)). The JERKZ algorithm also employs a two-step approach for IC detection, but without a maximum peak width criterion in the second pass, as the difference between the IC and mid-swing maxima is considerably larger.

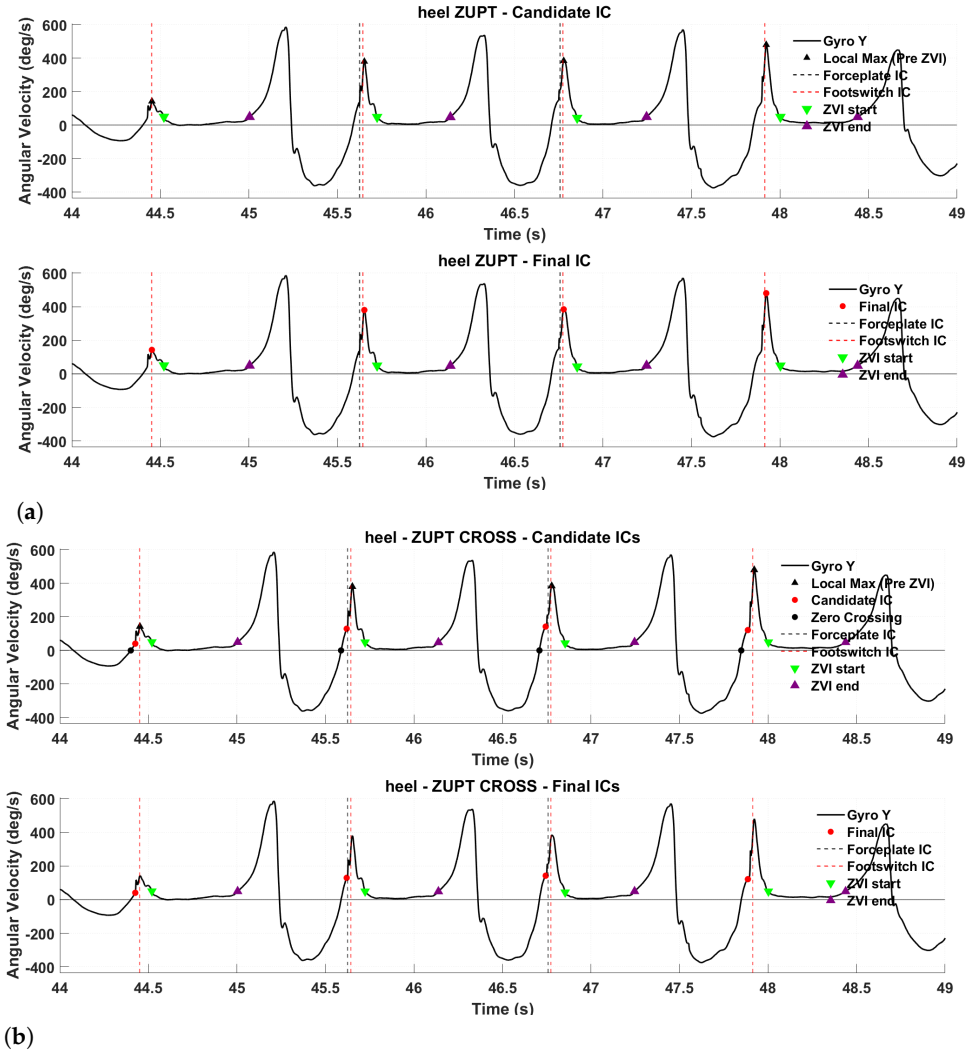

Figure 5. IMU-based initial-contact (IC) detection using the ZUPT method (a) and the ZUPT CROSS method (b). The ZUPT algorithm identifies ICs at the angular-velocity peak prior to the zero-velocity intervals. The ZUPT CROSS algorithm uses the zero crossing prior to the local angular velocity maximum and identifies the IC as the midway point between the two. In both panels, vertical dashed lines mark ground-truth ICs from foot-switches (red) and force plates (black). The top subplots show candidate ICs (black triangles) together with zero-velocity intervals (green and purple triangles); the bottom subplots display the final ICs (red dots) obtained after the second pass.

The third algorithm uses angular velocity in the sagittal plane as its target variable and is based on the zero-velocity update (ZUPT) method [17,29]. The ZUPT method identifies zero-velocity intervals (ZVIs) in

the sagittal angular velocity signal, which typically occur during mid-stance [30]. Visual inspection of the sagittal angular velocity signal, alongside force plate IC markings, revealed local maxima preceding these ZVIs near the reference IC instants (Figure 5(**a**)). In the implementation of this algorithm, ZVIs were defined as contiguous intervals lasting 0.15 to 1.0 s during which the absolute angular velocity remains below 50 deg/s. Then, the local maximum within the 0.3 s preceding the ZVI start is identified using MATLAB's findpeaks function and marked as a candidate IC. Consecutive IC candidates occurring within 0.6 to 1.7 s are retained as the final IC events.

The fourth detection algorithm, ZUPT CROSS, was derived from the ZUPT method. The modification was motivated by the observation that the force plate IC typically occurs before the local maximum in sagittal angular velocity, but after the the zero crossing. Therefore, ZUPT CROSS identifies IC candidates at the midpoint point in time between the zero-crossing preceding the local maximum, and the local maximum. The same second-pass criteria from the ZUPT algorithm were applied to to ZUPT CROSS.

2.6. Analysis

The IC events detected by the IMU-based systems were evaluated against the force plate reference in the laboratory trials, and against the footswitch reference ICs for the real-world trials. Additionally, the ICs detected with the footswitches in the laboratory trials were compared to the force plate reference. The datasets of the PWS and the fast paced walking speeds were combined for analysis. Detection performance was assessed based on detection accuracy and temporal agreement with the corresponding reference method.

2.6.1. Detection Accuracy

Detection accuracy was quantified using the F1-score as the primary performance metric, with recall and precision as intermediate measures. True positives (TP) were defined as correctly detected events, false positives (FP) as spurious detections, and false negatives (FN) as missed events. The F1-score, recall, and precision were calculated using equations (1), (2), and (3), respectively.

$$F_1 = 2 \times \frac{\text{Recall} \times \text{Precision}}{\text{Recall} + \text{Precision}} \quad (1) \qquad \text{Recall} = \frac{TP}{TP + FN} \quad (2) \qquad \text{Precision} = \frac{TP}{TP + FP} \quad (3)$$

2.6.2. Temporal Agreement

Temporal agreement was defined as the time difference between the detected IC and the reference IC event and calculated using equation (4).

$$\text{Error} = t_{\text{IC,IMU}} - t_{\text{IC,Ref}} \quad (4)$$

The primary performance metrics for temporal agreement were the mean and median detection errors, as well as the standard deviation (SD) and interquartile range (IQR) of the detection errors relative to the reference. The mean and median errors quantify the systematic bias, the SD and IQR quantify their temporal variability. Detection error distributions were tested for normality using the Lilliefors test, and statistical comparisons between systems were made using the Mann–Whitney U test (ranksum, MATLAB).

3. Results

3.1. Laboratory trials

A total of 404 force plate ICs were recorded during the laboratory walking trials at two walking speed conditions. These served as the ground-truth reference for evaluating the performance of both the footswitch- and IMU-based detection systems. Table 2 presents the detection accuracy and temporal agreement of each system with respect to the force plate ground truth. Systems with an F1-score $\geq$ 90% are ranked by ascending absolute mean error, systems below this threshold are listed in descending order of F1-score. The combination of the JERKZ algorithm and heel-mounted IMU achieved the highest temporal agreement with the fore plates, with a mean error of –1.5 ± 1.5 ms and an F1-score of 97.6%. In comparison, the insole footswitches had a significantly larger detection error of 17.7 ± 11.7 ms, despite a similar F1-score (97.2%).

Table 2. Detection performance of IMU-based and foot-switch systems in the laboratory trials (force-plate ground truth).

Detection System		Detection Accuracy (%)			Temporal Agreement (ms)		
Approach	Placement	F1	Recall	Precision	Mean ± SD	Median ± IQR	LOA
JERKZ	Heel	97.6	95.3	100.0	−1.5 ± 1.5	2.0 ± 2.0	[−4, 1]
ACCZ	Heel	99.8	99.5	100.0	−3.8 ± 1.5	0.0 ± 2.0	[−7, −1]
ZUPT CROSS	Heel	99.9	99.8	100.0	−4.5 ± 7.4	−2.0 ± 10.0	[−19, 10]
Footswitch	Insole	97.2	94.6	100.0	17.7 ± 11.7	16.9 ± 15.8	[−5, 41]
ZUPT	Instep	96.4	93.1	100.0	19.0 ± 17.8	36.0 ± 24.0	[−16, 54]
ZUPT CROSS	Instep	98.5	97.0	100.0	−19.0 ± 22.2	0.0 ± 30.0	[−63, 25]
ZUPT	Heel	99.9	99.8	100.0	23.9 ± 8.9	28.0 ± 12.0	[6, 41]
ACCZ	Low	85.7	75.0	100.0	33.2 ± 14.8	36.0 ± 20.0	[4, 62]
ZUPT CROSS	Low	80.1	66.8	100.0	13.6 ± 17.8	24.0 ± 24.0	[−21, 48]
ACCZ	Middle	78.3	64.4	100.0	36.5 ± 17.8	34.0 ± 24.0	[2, 71]

The ranking order is based on the absolute value of the mean error for systems with $F_1 \geq 90\%$, and on the F_1-score (descending) for systems with $F_1 < 90\%$.

The systems combining the heel mounted IMU with the JERKZ, ACCZ and ZUPT CROSS algorithms each had significantly lower detection errors compared to the insole footswitches ($p<0.01$), with mean errors of –1.5 ms to –4.5 ms versus 17.7 ms. The only system using the heel-mounted IMU that did not have a better temporal agreement with the force plates compared to the footswitches was the system that uses the ZUPT algorithm (23.9 ± 8.9 ms). The precision of each of the detection systems was 100% in the laboratory trials as there were no false positive detections, which means there were no spurious ICs detected in the forceplate IC intervals.

The distribution of the IC detection errors of each system in the laboratory trials is shown in figure 6. The JERKZ and ACCZ algorithms, both using the heel-mounted IMU, had the lowest median errors (2 ms and 0 ms, respectively) and the smallest IQRs (2 ms each). The footswitch system had a median error of 16.9 ms and a IQR of 15.8 ms.

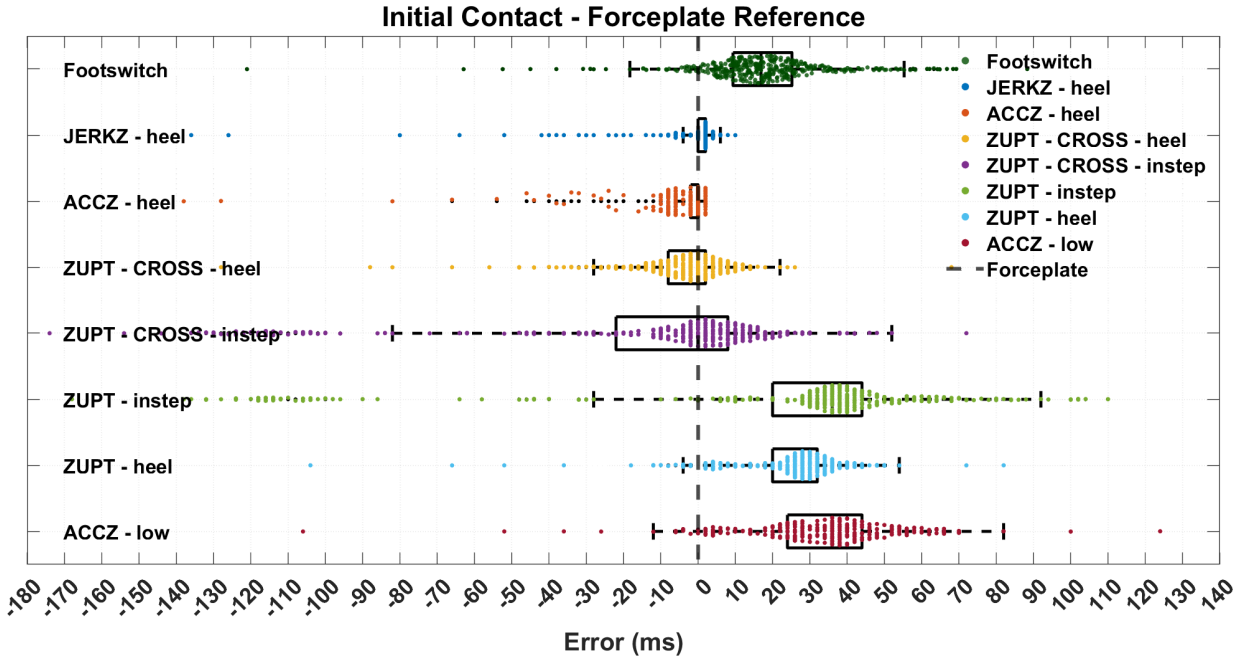

Figure 6. IC detection performance of the footswitches and IMU-based GED systems in the laboratory walking trials. The forceplate reference is marked with the vertical dashed line at t= 0 ms

3.2. Real-world trials

In the real-world trials, the footswitches served as the ground-truth reference. Table 3 presents the detection accuracy and temporal agreement of the IMU-based systems relative to the footswitches. The heel-mounted IMU yielded detection performance across all detection algorithms, followed by the instep, lower shank, and middle shank placements. The ZUPT algorithm combined with the heel placement achieved the highest temporal agreement with the footswitches (–5.0 ± 23.4 ms) and an F1-score of 92.6%. In terms of detection accuracy, the ACCZ algorithm combined with the heel placement had the highest F1-score (93.6 %). Among the systems not using a heel-mounted IMU, the ZUPT algorithm at the instep placement performed best, with an F1-score of 86.9% and a mean error of –12.8 ± 47.6 ms.

Table 3. IC detection performance of IMU-based GED systems in real-world environments (footswitch ground truth).

Detection System		Detection Accuracy (%)			Temporal Agreement (ms)		
Algorithm	**Placement**	**F1**	**Recall**	**Precision**	**Mean ± SD**	**Median ± IQR**	**LOA**
ZUPT	Heel	92.6	94.9	90.5	−5.0 ± 23.4	5.4 ± 31.6	[−51, 41]
JERKZ	Heel	91.0	90.2	91.9	−24.6 ± 16.5	−20.5 ± 22.3	[−57, 8]
ACCZ	Heel	93.6	96.4	90.9	−25.9 ± 15.5	−22.2 ± 20.9	[−56, 4]
ZUPT CROSS	Heel	91.8	93.1	90.5	−30.3 ± 18.6	−23.3 ± 25.1	[−67, 6]
ZUPT	Instep	86.9	86.4	87.5	−12.8 ± 47.6	15.4 ± 64.2	[−106, 80]
ZUPT CROSS	Instep	86.0	86.9	85.1	−45.0 ± 38.3	−22.9 ± 51.7	[−120, 30]
ACCZ	Low	77.7	68.3	90.0	14.4 ± 16.9	19.8 ± 22.8	[−19, 48]
ZUPT	Middle	76.8	63.3	97.4	21.5 ± 37.6	33.0 ± 50.8	[−52, 95]
ACCZ	Middle	73.8	58.7	99.3	14.6 ± 23.3	18.4 ± 31.5	[−31, 60]

The ranking order is based on the absolute value of the mean error for systems with $F_1 \geq 90\%$, and on the F_1-score (descending) for systems with $F_1 < 90\%$.

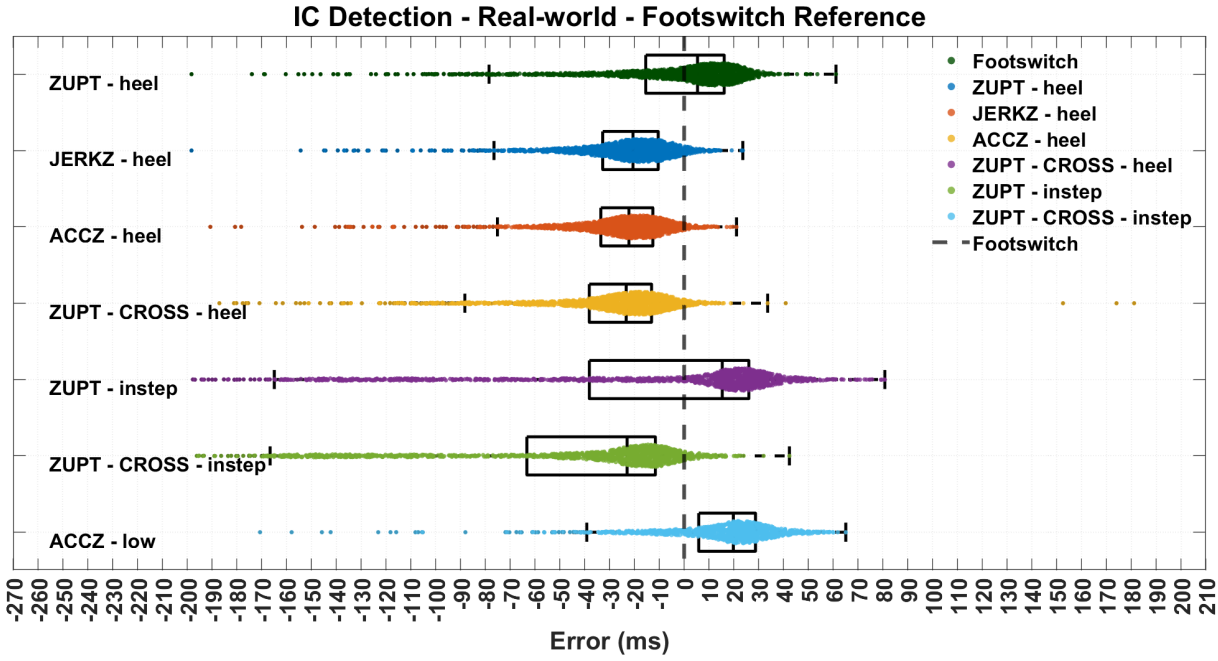

Figure 7. IC detection performance of IMU-based GED systems in real-world trials. The vertical dashed line at 0ms represents the footswitch reference.

4. Discussion

This study evaluated the feasibility of using IMU-based gait detection systems as an alternative to insole footswitches for collecting gait event datasets in real-world environments, particularly for training machine learning algorithms in wearable assistive devices. The detection performance of five IMU placement

locations and four detection algorithms was assessed in real-world settings using footswitches as the reference. Additionally, both the IMU-based systems and the footswitches were validated against force plates in laboratory settings (10N threshold), providing a comprehensive assessment of their detection accuracy and temporal precision. The results indicate that the heel is the most suitable placement location for IMU-based IC detection. In real-world trials, the combination of the heel-mounted IMU with the ZUPT, JERKZ, and ACCZ algorithms yielded high detection accuracies, with F1-scores of 92.6%, 91.0%, and 93.6%, respectively. Among these, the ZUPT algorithm demonstrated the best temporal agreement with the footswitch reference (mean error: –5.0 ± 23.4 ms). The laboratory trials, using force plates as the ground truth, confirmed that the IMU placement on the heel is the most suitable location for IC detection. The JERKZ and ACCZ algorithms, when combined with a heel-mounted IMU, achieved F1-scores of 97.6% and 99.8%, with mean temporal errors of –1.5 ± 1.5 ms and –3.8 ± 1.5 ms, respectively. Both systems also showed excellent temporal precision, with median errors of 0 ms and 2 ms, and interquartile ranges of 2 ms each. While the insole footswitch system achieved a comparable detection accuracy (97.2% F1-score), its temporal agreement with the force plate reference was significantly lower (mean error: 17.7 ± 11.7 ms; $p < 0.001$).

4.1. Interpretation in Relation to Previous Works

Several factors must be considered when interpreting the outcomes of this study in relation to related works, including differences in outcome metrics and reference methods. For instance, interpretation of studies using force plates references requires knowledge of the specific force threshold applied for IC detection [15,23]. Without this information, the reported temporal agreement with the evaluated system cannot be meaningfully interpreted, as the force threshold directly affects the detection timing of foot-ground contact. Moreover, temporal agreement should always be interpreted in conjunction with detection accuracy; as high temporal precision is limited value if the overall detection rate is low. Other considerations include the participant population, environment, and the type of walking tasks performed.

Previous studies have shown that for IMU-based IC detection, the foot and shoe are the best-performing sensor placement locations [17,25]. The outcomes of the present study are in line with these findings, as the heel and instep placements achieved the best IC detection performance in both the laboratory and real-world trials. Related studies in which footswitches were used for IC detection reported mean detection errors of 0 ± 3 ms (range -10, 8 ms) [26] and -2.7 ± 2.7 (% 95 CI -8 to 2.5 ms) [31]; both studies used force plates as ground truth reference. Another study [21] compared footswitch and IMU-based systems under varying walking speeds and algorithms, found that footswitches showed significantly better agreement with force plates than the best IMU-based method (RMSE: 2.4 ± 2.1 ms vs. 9.5 ± 9.0 ms; $p < 0.001$). The IMU-based method in that study used second derivative of fore-aft ankle acceleration. Compared to the present study, the IC detection performance of footswitches reported in [21,26,31] appears to be substantially better. The detection performances of footswitches reported in related studies is presented in Table 4 of the appendix. The interpretation of this discrepancy is challenging because [26] and [31] did not report detection accuracy. One likely explanation for the reduced temporal agreement is the footswitch force thresholds in the present study, which could have been set substantially higher to reduce spurious detections. Hence, a higher force threshold introduces a systematic delay in IC detection. However, this alone does not account for the higher variability observed (SD: 11.7 ms, IQR: 15.8 ms). Several factors may have contributed to this increased variability, including variations in surface compliance of the participants shoe soles and hardware issues that could have caused non-linear time jitters in the footswitch recordings. This increased variability in IC detection performance should be considered when evaluating the performance of the IMU-based detection systems in real-world environments, where the footswitches served as ground truth reference.

4.2. Limitations

Several limitations are acknowledged in this study. First, the variability of the footswitch detection performance relative to the force plate reference in the laboratory trials was substantial (SD = 11.7 ms, IQR = 16 ms). This raises concerns regarding the validity of using footswitches as a ground truth reference in the real-world trials. Nonetheless, when this variability is taken into account, the detection performance

of the heel-placed IMU-based systems can still be considered adequate for collecting training data in real-world environments. In fact, the variability of the best-performing IMU-based system in the real-world settings using the footswitches as reference (SD = 15.5 ms) was not substantially greater than that of the footswitches in the laboratory trials (11.7 ms). In contrast, the variability of this IMU-based detection system was substantially lower (SD = 1.5 ms). These findings suggest that the real-world detection performance of the IMU-based systems are likely underestimated due to the limited reliability of the footswitch reference. A major limitation of this study is the small sample size (n = 4), which resulted from hardware failure that restricted further data collection. Nonetheless, a substantial number of foot-ground contacts were analyzed in both the laboratory (404) and real-world trials ($\approx$ 6800), across both preferred and fast-paced walking speed conditions. The participants also represented a relatively diverse group, with ages ranging from 31 to 68 years and body weights between 64 and 81 kg. Another important limitation is that the cohort was limited to healthy adults. Consequently, it remains uncertain whether the findings in this work generalize to the target populations of wearable assistive devices. Future research should therefore assess the detection performance of these IMU-based systems in gait-impaired individuals. However, the results obtained from healthy adults provide an initial validation, demonstrating that IMU-based systems can achieve adequate detection performance in real-world environments. Moreover, the outcomes of this study indicate that the IC detection performance of IMU-based systems is superior to that of footswitch-based systems in healthy adults across the two walking speed conditions. Moreover, the findings of the present study have shown that in healthy-adults, IMU-based IC detection can out outperform footswitch-based IC detection across both walking speed conditions. Because the initial analysis did not reveal substantial differences in detection performance between the PWS and fast-paced walking speed conditions, the datasets were pooled to improve robustness of the analysis. The individual results for each walking speed were omitted for brevity. Additionally, the pooling of the two walking speed conditions increased the generalizability of the results to real-world environments, where the detection algorithms must perform reliably across varying walking speeds without speed-specific tuning.

Another limitation of the present study was the hardware constraints of the footswitch system, which prevented bilateral evaluation of IC detection. Because one of its connectors was used to synchronize the measurement systems, data collection was restricted to the participants' right legs. Furthermore, since synchronization between the IMU and footswitch systems was dependent on the laboratory setup, all real-world trials had to start in the laboratory. As a result, the out-of-lab conditions were combined into a single trial that included straight walking, turning, and obstacle negotiation. This prevented the individual assessment of the detection performance in specific aspects of walking in real-world environments. Future studies would benefit from separately analyzing distinct walking tasks and terrains to identify conditions under which real-world IC detection performance could be improved upon.

5. Conclusion

This study demonstrated that IMU-based IC detection using, a single heel-mounted sensor in combination with ACCZ, JERKZ, or ZUPT algorithms, outperformed footswitch-based detection in laboratory settings. Among the evaluated IMU placement locations, the heel was identified as the most effective for IC detection. In real-world environments, the heel-mounted IMU systems achieved F1-scores $\geq$ 92% relative to the footswitch reference. The ZUPT algorithm showed the best temporal agreement with the footswitches in real-world trials (-5.0 ms). However, the JERKZ algorithm is recommended for real-world IC detection due to its superior temporal agreement with the force plate reference and lower temporal variability in both laboratory and real-world settings. Moreover, the JERKZ algorithm was the most practical to implement, requiring minimal parameter tuning to maintain robust performance across walking conditions. It is concluded that a single heel-mounted IMU combined with a rule-based detection algorithm provides a viable alternative to insole footswitches for collecting gait datasets in real-world environments. This supports the development of wearable assistive devices by offering a practical and effective method for real-world gait event detection.

References

1. Jankovic, J. Gait Disorders. *Neurol. Clin.* **2015**, *33*, 249–268. https://doi.org/10.1016/j.ncl.2014.11.007.
2. Rueterbories, J.; Spaich, E.G.; Larsen, B.; Andersen, O.K. Methods for gait event detection and analysis in ambulatory systems. *Medical Engineering Physics* **2010**, *32*, 545–552. https://doi.org/10.1016/j.medengphy.2010.03.007.
3. Voisard, C.; de l'Escalopier, N.; Ricard, D.; Oudre, L. Automatic gait events detection with inertial measurement units: healthy subjects and moderate to severe impaired patients. *Journal of NeuroEngineering and Rehabilitation* **2024**, *21*, 104.
4. Prasanth, H.; Caban, M.; Keller, U.; Courtine, G.; Ijspeert, A.; Vallery, H.; von Zitzewitz, J. Wearable Sensor-Based Real-Time Gait Detection: A Systematic Review. *Sensors* **2021**, *21*, 2727. https://doi.org/10.3390/s21082727.
5. Hulleck, A.A.; Mohan, D.M.; Abdallah, N.; Rich, M.E.; Khalaf, K. Present and future of gait assessment in clinical practice: Towards the application of novel trends and technologies. *Frontiers in Medical Technology* **2022**, *4*, 901331. https://doi.org/10.3389/FMEDT.2022.901331.
6. Gao, S.; Chen, J.; Dai, Y.; Hu, B. *Wearable Systems Based Gait Monitoring and Analysis*, 1 ed.; Springer International Publishing: Cham, Switzerland, 2022; pp. 1–238. https://doi.org/10.1007/978-3-030-97332-2.
7. Rokhmanova, N.; Pearl, O.; Kuchenbecker, K.J.; Halilaj, E. IMU-Based Kinematics Estimation Accuracy Affects Gait Retraining Using Vibrotactile Cues. *IEEE Transactions on Neural Systems and Rehabilitation Engineering* **2024**, *32*, 1005–1012. https://doi.org/10.1109/TNSRE.2024.3365204.
8. Vu, H.T.T.; Dong, D.; Cao, H.L.; Verstraten, T.; Lefeber, D.; Vanderborght, B.; Geeroms, J. A Review of Gait Phase Detection Algorithms for Lower Limb Prostheses. *Sensors* **2020**, *20*, 3972. https://doi.org/10.3390/s20143972.
9. Gonzalez-Gutierrez, E.; Mercado-Gutierrez, J.A.; Yanez-Suarez, O., An Exploration on the Use of IMUs for Real-Time Detection of Gait Events, Towards Closed-Loop Gait Rehabilitation Based on Functional Electrical Stimulation. In *IFMBE Proceedings*; Springer Science and Business Media Deutschland GmbH, 2025; Vol. 116 IFMBE, pp. 293–303. https://doi.org/10.1007/978-3-031-82123-3_28.
10. Chung, Y.; Kim, J.H.; Cha, Y.; Hwang, S. Therapeutic Effect of Functional Electrical Stimulation-Triggered Gait Training Corresponding to Gait Cycle for Stroke. *Gait & Posture* **2014**, *40*, 471–475. https://doi.org/10.1016/j.gaitpost.2014.03.010.
11. Donlin, M.C.; Higginson, J.S. Adaptive Functional Electrical Stimulation Delivers Stimulation Amplitudes Based on Real-Time Gait Biomechanics. *Journal of Medical Devices* **2024**, *18*.
12. Gouda, A.; Andrysek, J. Rules-Based Real-Time Gait Event Detection Algorithm for Lower-Limb Prosthesis Users during Level-Ground and Ramp Walking. *Sensors* **2022**, *22*, 8888. https://doi.org/10.3390/s22228888.
13. Lu, Y.; Zhu, J.; Chen, W.; Ma, X. Inertial Measurement Unit-Based Real-Time Adaptive Algorithm for Human Walking Pattern and Gait Event Detection. *Electronics 2023, Vol. 12, Page 4319* **2023**, *12*, 4319. https://doi.org/10.3390/ELECTRONICS12204319.
14. Schofield, J.S.; Evans, K.R.; Hebert, J.S.; Marasco, P.D.; Carey, J.P. The effect of biomechanical variables on force sensitive resistor error: Implications for calibration and improved accuracy. *Journal of biomechanics* **2016**, *49*, 786–792.
15. Hanlon, M.; Anderson, R. Real-time gait event detection using wearable sensors. *Gait & Posture* **2009**, *30*, 523–527. https://doi.org/10.1016/j.gaitpost.2009.07.128.
16. Havashinezhadian, S.; Chiasson-Poirier, L.; Sylvestre, J.; Turcot, K. Inertial Sensor Location for Ground Reaction Force and Gait Event Detection Using Reservoir Computing in Gait. *International Journal of Environmental Research and Public Health* **2023**, *20*, 3120. https://doi.org/10.3390/ijerph20043120.
17. Niswander, W.; Kontson, K. Evaluating the Impact of IMU Sensor Location and Walking Task on Accuracy of Gait Event Detection Algorithms. *Sensors* **2021**, *21*, 3989. https://doi.org/10.3390/s21123989.
18. Panebianco, G.P.; Bisi, M.C.; Stagni, R.; Fantozzi, S. Validation of IMU-Based Gait Event Detection during Curved Walking and Turning in Healthy Older Adults. *Journal of NeuroEngineering and Rehabilitation* **2021**, *18*, 28. https://doi.org/10.1186/s12984-021-00828-0.
19. Salminen, M.; Perttunen, J.; Avela, J.; Vehkaoja, A. Comparative assessment of heel rise detection for consistent gait phase separation. *Heliyon* **2024**, *10*, e33546. https://doi.org/10.1016/j.heliyon.2024.e33546.
20. Delfi, G.; Al Bochi, A.; Dutta, T. A scoping review on minimum foot clearance measurement: Sensing modalities. *International journal of environmental research and public health* **2021**, *18*, 10848.
21. Hanlon, M.; Anderson, R. Real-time gait event detection using wearable sensors. *Gait & posture* **2009**, *30*, 523–527.
22. Romijnders, R.; Warmerdam, E.; Hansen, C.; Schmidt, G.; Maetzler, W. A Deep Learning Approach for Gait Event Detection from a Single Shank-Worn IMU: Validation in Healthy and Neurological Cohorts. *Sensors* **2022**, *22*. https://doi.org/10.3390/s22103859.

23. Tirosh, O.; Sparrow, W. Identifying heel contact and toe-off using forceplate thresholds with a range of digital-filter cutoff frequencies. *Journal of Applied Biomechanics* **2003**, *19*, 178–184.
24. Ben Mansour, K.; Rezzoug, N.; Gorce, P. Analysis of several methods and inertial sensors locations to assess gait parameters in able-bodied subjects. *Gait & Posture* **2015**, *42*, 409–414. https://doi.org/10.1016/j.gaitpost.2015.05.020.
25. Panebianco, G.P.; Bisi, M.C.; Stagni, R.; Fantozzi, S. Analysis of the performance of 17 algorithms from a systematic review: Influence of sensor position, analysed variable and computational approach in gait timing estimation from IMU measurements. *Gait & Posture* **2018**, *66*, 76–82. https://doi.org/10.1016/j.gaitpost.2018.08.025.
26. Hausdorff, J.M.; Ladin, Z.; Wei, J.Y. Footswitch system for measurement of the temporal parameters of gait. *Journal of biomechanics* **1995**, *28*, 347–351.
27. Hreljac, A.; Marshall, R.N. Algorithms to determine event timing during normal walking using kinematic data. *Journal of Biomechanics* **2000**, *33*, 783–786. https://doi.org/10.1016/S0021-9290(00)00014-2.
28. Patterson, M.R.; Johnston, W.; O'Mahony, N.; O'Mahony, S.; Nolan, E.; Caulfield, B. Validation of temporal gait metrics from three IMU locations to the gold standard force plate. In Proceedings of the 2016 38th Annual International Conference of the IEEE Engineering in Medicine and Biology Society (EMBC). IEEE, 2016, pp. 667–671. https://doi.org/10.1109/EMBC.2016.7590790.
29. Foxlin, E. Pedestrian tracking with shoe-mounted inertial sensors. *IEEE Computer graphics and applications* **2005**, *25*, 38–46.
30. Wahlström, J.; Skog, I. Fifteen years of progress at zero velocity: A review. *IEEE Sensors Journal* **2020**, *21*, 1139–1151.
31. Mills, P.M.; Barrett, R.S.; Morrison, S. Agreement between footswitch and ground reaction force techniques for identifying gait events: Inter-session repeatability and the effect of walking speed. *Gait & posture* **2007**, *26*, 323–326.
32. Wall, J.C.; Crosbie, J. Accuracy and reliability of temporal gait measurement. *Gait & Posture* **1996**, *4*, 293–296. https://doi.org/10.1016/0966-6362(95)01049-6.
33. Han, Y.C.; Wong, K.I.; Murray, I. Gait Phase Detection for Normal and Abnormal Gaits Using IMU. *IEEE Sensors Journal* **2019**, *19*, 3439–3448. https://doi.org/10.1109/JSEN.2019.2894143.
34. Pradeau, C.; Sturbois-Nachef, N.; Allart, E.; Pillet, M.; Thevenon, A. Concurrent validity of the ZeroWire® footswitch system for the measurement of temporal gait parameters. *Gait & Posture* **2020**, *82*, 133–137. https://doi.org/10.1016/j.gaitpost.2020.09.015.
35. Neumann, S.; Bauer, C.M.; Nastasi, L.; Albensi, C.B.; Alimusaj, M.; Theilmeier, A.; Gollhofer, A.; Bretthauer, G. Accuracy, concurrent validity, and test–retest reliability of pressure-based insoles for gait measurement in chronic stroke patients. *Frontiers in Digital Health* **2023**, *5*, 1162696. https://doi.org/10.3389/fdgth.2023.1162696.
36. Parati, M.; Gallotta, M.; Muletti, M.; Bovi, G.; Rinaldi, F.; Cereatti, A.; Della Croce, U. Validation of pressure-sensing insoles in patients with Parkinson's disease during overground walking in single and cognitive dual-task conditions. *Sensors* **2022**, *22*, 6392. https://doi.org/10.3390/s22176392.
37. Blades, S.; Marriott, H.; Hundza, S.; Barakzai, E.; MacNeil, J.; Bruening, T.E. Evaluation of different pressure-based foot contact event detection algorithms across different slopes and speeds. *Sensors* **2023**, *23*, 2736. https://doi.org/10.3390/s23052736.
38. Storm, F.A.; Buckley, C.J.; Mazzà, C. Gait event detection in laboratory and real life settings: Accuracy of ankle and waist sensor based methods. *Gait & posture* **2016**, *50*, 42–46.

Acknowledgments: The author gratefully acknowledges the valuable feedback and insightful suggestions provided by Dr. Eline van der Kruk, Ir. Koen Jongbloed, and Dr. Lance Rane, as well as the technical support from Jacques Brenkman. Sincere gratitude is extended to my family and friends for their continuous encouragement and support. Special thanks are due to Dr. Jim Boonman, Ir. Nihar Sabnis, Ir. Alvaro Assis de Souza and Stef Beijk.

Author	Citation	Year	N	Population	Event	Accuracy	Time Agreement	Ref.
Hausdorff et al.	[26]	1995	10	Healthy	IC	Not reported	Mean ± SD: 0 ± 3 ms Range: (-10 ms, 8 ms)	Forceplate (10 N)
Wall & Crosbie	[32]	1996	–	Healthy	HS	100% detection rate	10–20 ms	OMC
Mills et al.	[31]	2007	10	Healthy	HS	Not reported	Mean ± SD: -2.7 ± 2.7 95% CI: -8 ms to 2.5 ms	Forceplate
Hanlon & Anderson	[33]	2009	12	Healthy	HS	Precision: 98%, Recall: 96%, FP: 2%	Mean Absolute Error 2.4 ± 2.1 ms RMSE: 5.1 ms	Forceplate (5N)
Pradeau et al.	[34]	2020	40	Healthy	HS	ICC > 0.91	Mean: 0.00–0.01 s LOA: 20 ms	GAITRite
Neumann et al.	[35]	2024	17	Post-stroke	HS	Precision: 100%, Recall: 99.4%, FP: 0%	Mean: -0.01 s RMSE: 11 ms	OMC
Parati et al.	[36]	2022	20	Parkinson's	HS	–	–	GAITRite
Blades et al.	[37]	2023	–	Healthy	HS	Best algorithm: 99%	Mean: 2–5 ms (level)	Ins Treadmill

Table 4. Comparison of Insole Footswitch/Pressure Sensor Systems vs. Gold-Standard References
(Only HS detection results are displayed.)
Abbreviations: HS = Heel Strike, OMC = Optical Motion Capture, SD = Standard Deviation, RMSE = Root Mean Square Error, LOA = Limits of Agreement, ICC = Intraclass Correlation.

Author	Year	N	Population	Placement	Signal Type	Algorithm Type	Performance Metrics
Romijnders et al. [22]	2022	157	Healthy & Neurological	Foot	Acc+Gyro	Deep Learning (TCN)	IC: 0 ms (median); TO: 5 ms (median) (Ref: OMC)
Storm [38]	2016	–	Healthy	Shank	Acc+Gyro	Threshold-Based	IC: <15 ms; TO: 28–51 ms; Stance: 30–50 ms (Ref: Pressure Insoles)
Garcia (2022)	2022	–	Healthy	Thigh	Acc	Adaptive Threshold	IC: 36.7 ms; TO: +6.7 ms (Ref: OMC)
Niswander et al. [17]	2021	7	Healthy Adults	Shank - Lateral	Acc+Gyro	MLvel/APacc	Stance: 17.9 $\pm$ 13.2 ms (Ref: Pressure Walkway)
				Shank - Lower		MLvel/APacc	Stance: 22 $\pm$ 18.7 ms
				Shin		MLvel/APacc	Stance: 32.4 $\pm$ 24.5 ms
				Shoe - Heel		APacc/MLvel	Stance: 44.9 $\pm$ 15.5 ms
				Shoe - Instep		SIacc/APacc	Stance: 34.4 $\pm$ 21 ms

Table 5. IMU-Based Gait Event Detection Performance by Sensor Placement and Study.
Abbreviations: HS = Heel Strike, TO = Toe-Off, IC = Initial Contact, FC = Final Contact, Acc = Accelerometer, Gyro = Gyroscope, LoA = Limits of Agreement, PD = Parkinson's Disease, OA = Osteoarthritis, OMC = Optical Motion Capture.

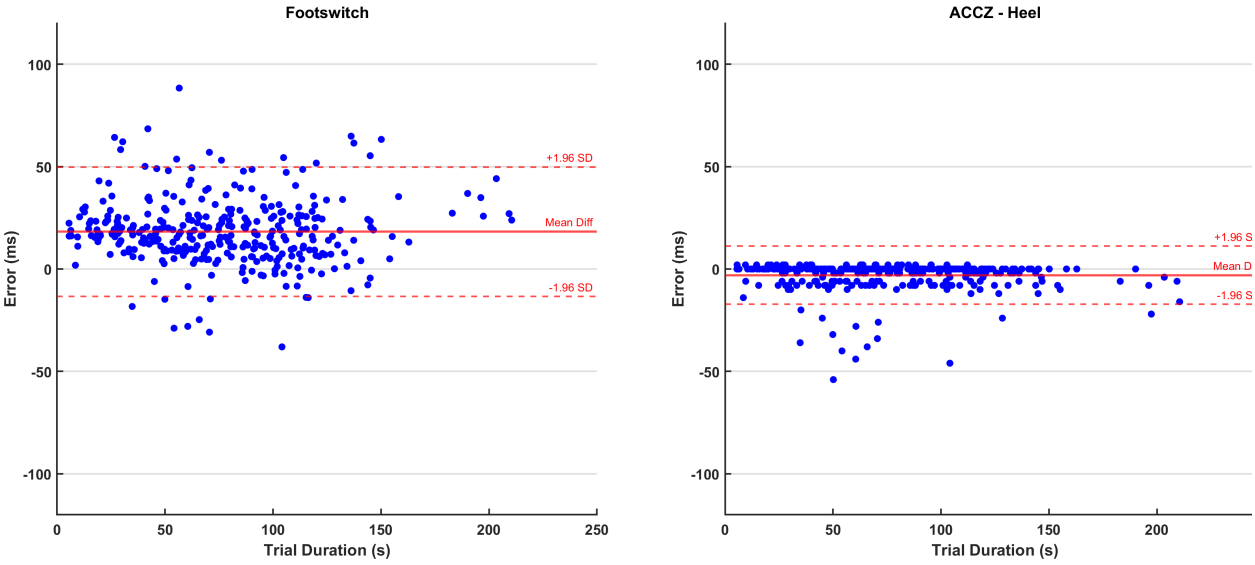

Figure 8. Bland-Altman plots of the IC detection of the Footswitches and the ACCZ heel IMU-based GED